Photochemical Phase Transition Behavior of Highly Birefringent Azotolane Liquid-Crystalline Polymer Films: Effects of the Position of the Tolane Group and the Donor−Acceptor Substituent in the Mesogen

Kunihiko Okano, Atsushi Shishido, and Tomiki Ikeda*

Chemical Resources Laboratory, Tokyo Institute of Technology, R1-11, 4259 Nagatsuta, Midori-ku, Yokohama 226-8503, Japan

Received June 18, 2005; Revised Manuscript Received October 17, 2005

ABSTRACT: Highly birefringent liquid-crystalline polymers (LCPs) containing an azobenzene group directly connected to a tolane moiety (azotolane moiety) were synthesized. Attention was focused on the effect of the position of the tolane moiety in the mesogenic azotolane group and the donor−acceptor substituent on photochemical phase transition behavior. In solution, cis−trans back-isomerization of the LCP containing azotolane moieties with a donor−acceptor was faster than that of LCPs having no acceptor groups. All the LCP films showed a homogeneous alignment and very high values of birefringence (about 0.4 at 633 nm). In the LCPs with a conventional azotolane moiety, a large change in birefringence (above 0.35) was induced repeatedly by irradiation of UV light. Furthermore, we investigated photoswitching behavior at telecommunication wavelength (1550 nm) based on the photochemical phase transition by irradiation of UV light.

Introduction

Azo-dye-containing compounds, in which a change in birefringence (Δn) can be induced by photoisomerization, are promising materials for photonic applications.[1−4] A large change in Δn enables a large change in the phase of incident light, which is very useful and effective for optical materials. For various azobenzene compounds, we have performed so far systematic studies on the nematic−isotropic (N−I) phase transition of azobenzene liquid-crystalline polymers (LCPs).[5] An advantage of the azobenzene LCPs is the fact that a large change in Δn is induced quickly by photoisomerizaition of the azobenzene moieties.[6,7] In the azobenzene LCPs, the azobenzene moiety in a trans form, which is rodlike, stabilizes the phase structure of the LC phase. On the other hand, the cis isomer shows a bent shape and destabilizes the LC phase. Consequently, trans−cis photoisomerization of the azobenzene chromophores leads to a large change in Δn by disorganizing the alignment of the LC phase. It has also been known that polarized light can induce birefringence due to the photoinduced change in alignment of the azobenzene moieties through trans−cis−trans isomerization cycles.[8,9] Moreover, polymer films have many advantages for practical application such as stability of optical storage and good mechanical properties. Therefore, a class of polymers containing an azobenzene moiety is a candidate for high-density optical recording as well as holographic and multibit recording,[10−12] photoswitching,[6,7] and nolinear optical materials.[13] To develop a high-performance optical material using azobenzene polymers, it is necessary to induce a large change in Δn by light.

The aim of this work is to synthesize highly birefringent LCPs containing a long mesogenic core in which the azobenzene group is directly connected to the tolane moiety (azotolane moiety) because tolanes are well-known as highly birefringent mesogens.[14−16] Although Yang et al. reported the synthesis of low-molecular-weight azotolanes and their thermotropic properties, they explored no photoresponsive behavior of these compounds.[17] In this study, we synthesized highly birefringent LCPs containing azotolane moieties and characterized in detail their LC behavior. Furthermore, we explored the photoisomerization behavior of the azobenzene moieties directly attached to the tolane moieties and the consequent change in alignment of the azotolane chromophores, leading to a change in Δn. We paid special attention to the effects of the position of the tolane moietiy in the mesogenic azotolane group and the donor−acceptor moiety on the photoisomerization behavior.

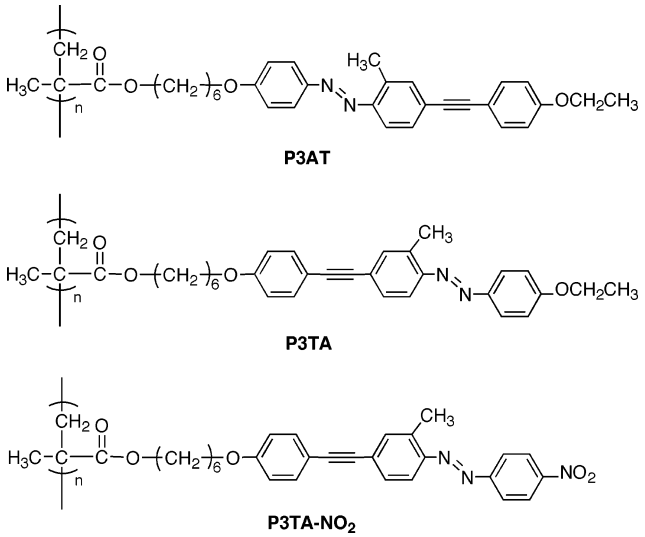

Figure 1. Structures of the LCPs used in this study and their abbreviations.

Experimental Section

Materials. Figure 1 shows the structures of LCPs as well as their abbreviations used in this study. **P3AT** was prepared according to the previously reported procedure.[18] The synthesis of polymers **P3TA** and **P3TA-NO$_2$** is outlined in Schemes 1 and 2. The compounds **1**, **2**, **5**, and **10** were prepared using a procedure similar to the literature.[19,20]

* Corresponding author. E-mail: tikeda@res.titech.ac.jp.

10.1021/ma0512814 CCC: $33.50
Published on Web 11/30/2005

Scheme 1

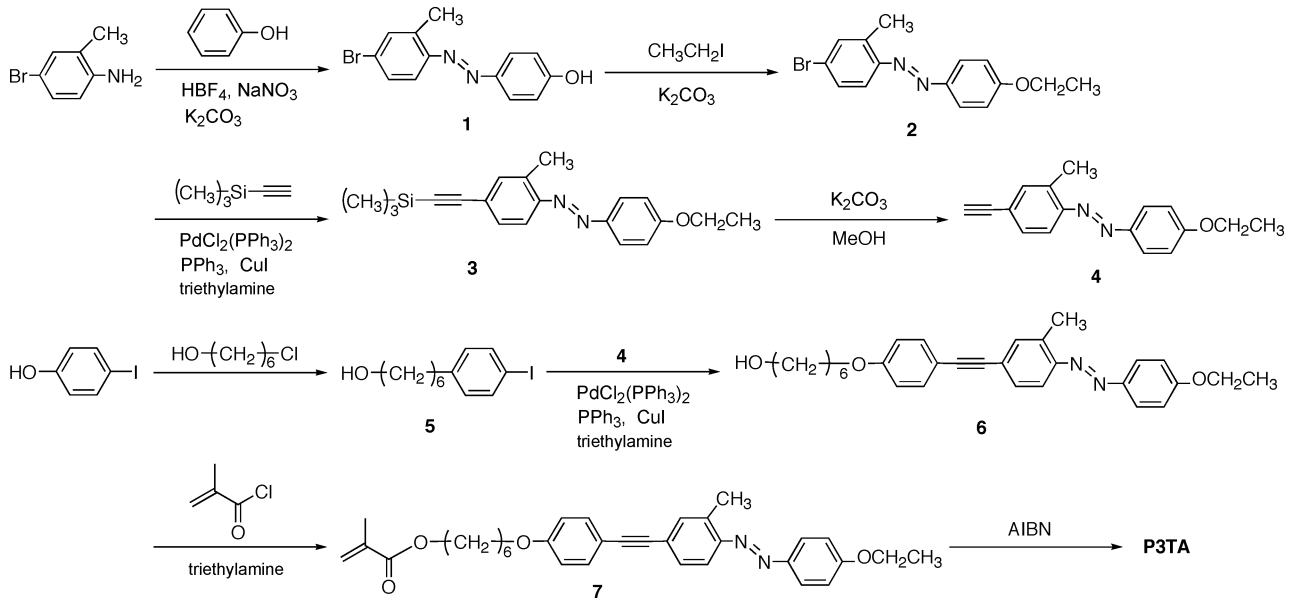

Scheme 2

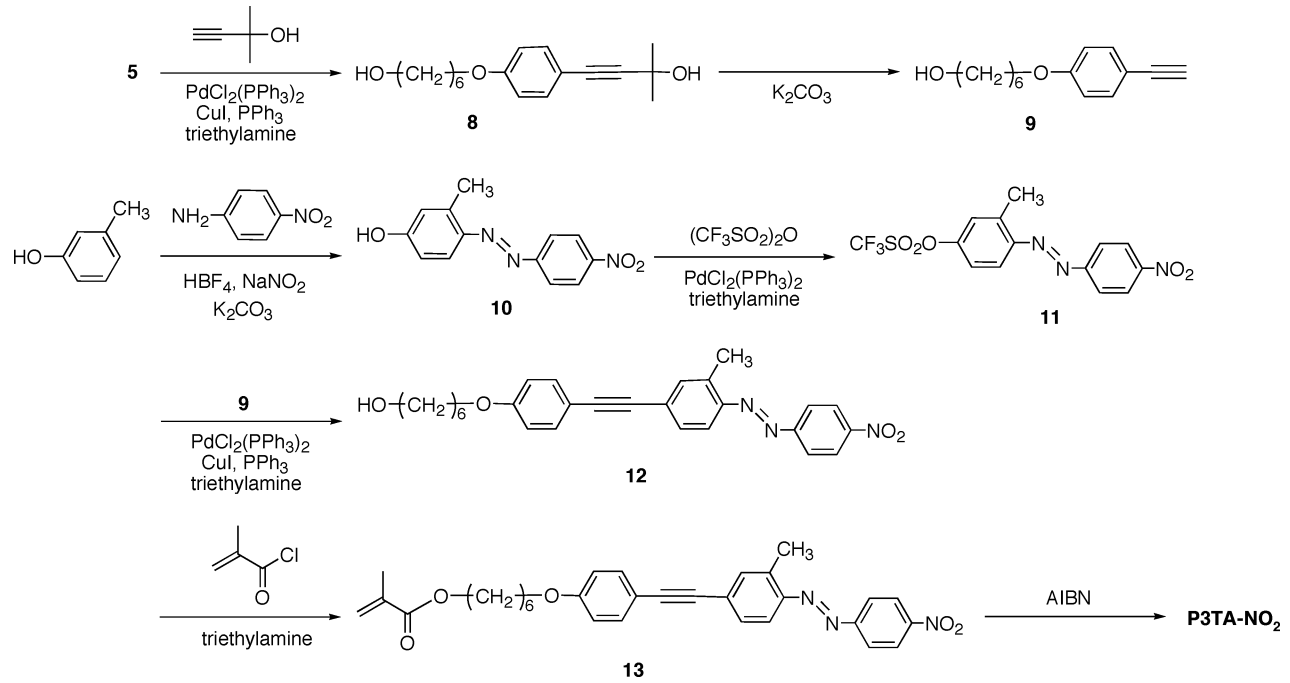

4-Ethoxy-2′-methyl-4′-(trimethylsilylethynyl)azobenzene (3). Compound **2** (6.7 g, 21 mmol), trimethylsilylacetylene (3.9 g, 40 mmol), $PdCl_2(PPh_3)_2$ (0.70 g, 1.0 mmol), CuI (0.70 g, 3.7 mmol), and PPh_3 (1.3 g, 5.0 mmol) were dissolved in triethylamine (20 mL) and THF (20 mL). The mixture was stirred at 60 °C for 8 h under a nitrogen atmosphere. The resulting solution was cooled to room temperature and extracted with ethyl acetate. After the organic layer was dried with anhydrous magnesium sulfate, the solvent was removed by evaporation. The product was purified by column chromatogrqaphy (silica gel, ethyl acetate:chloroform = 1:1 as eluent) to yield 6.0 g (90%) of orange powder. ^{1}H NMR ($CDCl_3$, δ, ppm): 0.25 (s, 9H), 1.44 (t, J = 7.2 Hz, 3H), 2.64 (s, 3H), 4.13 (q, J = 6.9 Hz, 2H), 6.98 (d, J = 8.7 Hz, 2H), 7.32−7.59 (m, 3H), 7.88 (d, J = 8.7 Hz, 2H).

4-Ethoxy-2′-methyl-4′-ethynylazobenzene (4). Compound **3** (6.0 g, 18 mmol) and K_2CO_3 (0.1 g) were stirred in a mixture of THF (20 mL) and methanol (200 mL) for 3 h at room temperature. The mixture was extracted with ethyl acetate. After the organic layer was dried with anhydrous magnesium sulfate, the solvent was removed by evaporation. The product was purified by column chromatogrqaphy (silica gel, ethyl acetate:chloroform = 1:1 as eluent) to yield 4.2 g (90%) of orange powder. ^{1}H NMR ($CDCl_3$, δ, ppm): 1.45 (t, J = 7.2 Hz, 3H), 2.64 (s, 3H), 3.19 (s, 1H), 4.14 (q, J = 6.9 Hz, 2H), 6.98 (d, J = 8.7 Hz, 2H), 7.32−7.57 (m, 3H), 7.89 (d, J = 8.7 Hz, 2H).

4-Ethoxy-2′-methyl-4′-(6-hydroxyhexyloxyphenylethynyl)-azobenzene (6). Compound **5** (2.8 g, 9.1 mmol), compound **4** (2.0 g, 7.6 mmol), $PdCl_2(PPh_3)_2$ (0.27 g, 0.38 mmol), CuI (0.27 g, 0.98 mmol), and PPh_3 (0.37 g, 1.9 mmol) were dissolved in triethylamine (30 mL) and THF (30 mL). The mixture was stirred at 60 °C for 8 h under a nitrogen atmosphere. The resulting solution was cooled to room temperature and extracted with ethyl acetate. After the organic layer was dried with anhydrous magnesium sulfate, the solvent was removed by evaporation. The product was purified by column chromatogrqaphy (silica gel, ethyl acetate:hexane = 1:1 as eluent) to yield 2.0 g (58%) of orange powder. ^{1}H NMR ($CDCl_3$, δ, ppm): 1.43−1.85 (m, 8H), 1.93 (s, 3H), 2.66 (s, 3H), 4.02−4.18 (m, 4H), 5.54 (s, 1H), 6.09 (s, 1H), 6.85 (d, J = 8.8 Hz, 2H),

6.98 (d, $J = 8.7$ Hz, 2H), 7.35−7.46 (m, 3H), 7.59 (d, $J = 8.4$ Hz, 2H), 7.89 (d, $J = 8.7$ Hz, 2H).

6-[4-[3-Methyl-4-(4-ethoxyphenylazo)ethynylphenoxy]hexyl Methacrylate (7). A solution of methacryloyl chloride (0.92 g, 8.8 mmol) in THF (30 mL) was added dropwise at 0 °C to a mixture of compound **6** (2.0 g, 4.4 mmol), triethylamine (0.89 g, 8.8 mmol), and a trace amount of hydroquinone, and the reaction mixture was stirred at room temperature for 24 h. The solution was poured into saturated aqueous sodium hydrogen carbonate, and the product was extracted with ethyl acetate. After the organic layer was dried with anhydrous magnesium sulfate, the solvent was removed by evaporation. The crude solid was purified by column chromatography (silica gel, chloroform as eluent) and finally recrystallized from methanol to yield 0.80 g (34%) of an orange solid. ^{1}H NMR ($CDCl_3$, δ, ppm): 1.37−1.82 (m, 8H), 2.67 (s, 3H), 3.69 (q, $J = 6.9$ Hz, 2H), 3.96 (t, $J = 6.9$ Hz, 2H), 6.98 (d, $J = 8.4$ Hz, 2H), 7.32−7.50 (m, 3H), 7.59 (d, $J = 8.4$ Hz, 2H), 7.89 (d, $J = 8.7$ Hz, 2H). ^{13}C NMR: 14.66, 17.33, 18.24, 25.70, 28.47, 29.00, 63.41, 64.53, 65.03, 68.03, 88.18, 91.44, 114.45, 114.59, 115.35, 124.81, 125.17, 125.37, 129.49, 133.04, 133.96, 136.39, 137.63, 147.31, 149.80, 159.08, 161.50, 167.40. MS (FAB): 525 (MH^+). Anal. Calcd for $C_{33}H_{36}N_2O_4$: C, 75.54; H, 6.92; N, 5.34. Found: C, 75.78; H, 7.14; N, 5.29.

Polymerization of Monomer 7. Compound **7** (0.80 g, 1.5 mmol) and AIBN (2.3 mg, 14 μmol) were dissolved in dry DMF (8 mL) and placed in a polymerization tube. After several freeze−pump−thaw cycles, the tube was sealed under high vacuum. Then, the tube was kept at 60 °C for 48 h. The resulting solution was cooled to room temperature and poured into 400 mL of methanol with vigorous stirring to precipitate the polymer. The polymer obtained was purified by repeated reprecipitation from DMF into a large excess of methanol and dried under vacuum for 48 h to yield 0.50 g of **P3TA** in 63% conversion.

4-(3-Hydroxy-3-methyl-1-butynyl)-(6-hydroxyhexyloxy)benzene (8). Compound **5** (15 g, 21 mmol), 2-methyl-3-butyn-2-ol (7.9 g, 94 mmol), $PdCl_2(PPh_3)_2$ (1.6 g, 2.3 mmol), CuI (1.6 g, 8.4 mmol), and PPh_3 (3.0 g, 11.5 mmol) were dissolved in triethylamine (50 mL) and THF (50 mL). The mixture was stirred at 60 °C for 8 h under a nitrogen atmosphere. The resulting solution was cooled to room temperature and extracted with ethyl acetate. After the organic layer was dried with anhydrous magnesium sulfate, the solvent was removed by evaporation. The product was purified by column chromatography (silica gel, ethyl acetate:hexane = 1:1 as eluent) to yield 8.7 g (70%) of a brown solid. ^{1}H NMR ($CDCl_3$, δ, ppm): 1.38−1.84 (m, 10H), 2.02 (s, 3H), 3.63 (t, $J = 6.6$ Hz, 2H), 3.92 (t, $J = 6.6$ Hz, 2H), 6.78 (d, $J = 8.9$ Hz, 2H), 7.30 (d, $J = 8.7$ Hz, 2H).

4-Ethynyl-(6-hydroxyhexyloxy)benzene (9). A solution of compound **8** (3.6 g, 13 mmol) and NaOH (0.5 g) in methanol was stirred for 3 h at 100 °C under nitrogen. The mixture was cooled to room temperature and extracted with ethyl acetate. After the organic layer was dried with anhydrous magnesium sulfate, the solvent was removed by evaporation. The product was purified by column chromatogrqaphy (silica gel, ethyl acetate:hexane = 1:1 as eluent) to yield 2.0 g (70%) of orange powder. ^{1}H NMR ($CDCl_3$, δ, ppm): 1.26−1.73 (m, 10H), 2.87 (s, 1H), 3.65 (t, $J = 6.6$ Hz, 2H), 3.84 (t, $J = 6.6$ Hz, 2H), 6.71 (d, $J = 8.7$ Hz, 2H), 7.29 (d, $J = 8.7$ Hz, 2H).

4-Nitro-2′-methyl-4′-[[(trifluoromethyl)sulfonyl]oxy]azobenzene (11). A solution of compound **10** (6.5 g, 25 mmol), pyridine (4.3 g, 54 mmol), and 4-(dimethylamino)pyridine (0.1 g) in chloroform (40 mL) was deaerated with nitrogen. Anhydrous trifluoromethanesulfonic acid (6.0 g, 20 mmol) in chloroform (10 mL) was added dropwise to the mixture and stirred at 0 °C for 3 h. The organic layer was extracted with ethyl acetate and washed with water twice. The product was purified by column chromatogrqaphy (silica gel, ethyl acetate:hexane = 1:1 as eluent) to yield 6.1 g (80%) of orange powder. ^{1}H NMR ($CDCl_3$, δ, ppm): 1.23 (s, 3H), 2.79 (s, 3H), 7.20 (d, $J = 8.7$ Hz, 1H), 7.29 (s, 1H), 7.83 (d, $J = 8.7$ Hz, 1H), 7.80 (d, $J = 8.7$ Hz, 2H), 8.41 (d, $J = 8.7$ Hz, 2H).

4-Nitro-2′-methyl-4′-(6-hydroxyhexyloxyphenylethynyl)azobenzene (12). Compound **11** (2.9 g, 7.3 mmol), compound **9** (1.6 g, 7.3 mmol), $PdCl_2(PPh_3)_2$ (0.26 g, 0.37 mmol), CuI (0.26 g, 1.4 mmol), and PPh_3 (0.49 g, 1.9 mmol) were dissolved in triethylamine (30 mL) and THF (30 mL). The mixture was stirred at 60 °C for 8 h under a nitrogen atmosphere. The resulting solution was cooled to room temperature and extracted with ethyl acetate. After the organic layer was dried with anhydrous magnesium sulfate, the solvent was removed by evaporation. The product was purified by column chromatogrqaphy (silica gel, ethyl acetate:hexane = 1:1 as eluent) to yield 2.1 g (63%) of orange powder. ^{1}H NMR ($CDCl_3$, δ, ppm): 1.46−1.94 (m, 8H), 2.74 (s, 3H), 3.65 (t, $J = 6.3$ Hz, 3H), 3.97 (t, $J = 6.3$ Hz, 3H), 6.87 (d, $J = 8.6$ Hz, 2H), 7.26−7.69 (m, 5H), 8.00 (d, $J = 8.7$ Hz, 2H), 8.36 (d, $J = 8.8$ Hz, 2H).

6-[4-[3-Methyl-4-(4-nitrophenylazo)phenylethynylphenoxy]-hexyl Methacrylate (13). A solution of methacryloyl chloride (0.37 g, 3.6 mmol) in THF (30 mL) was added dropwise at 0 °C to a mixture of compound **12** (0.89 g, 1.8 mmol), triethylamine (0.37 g, 3.6 mmol), and a trace amount of hydroquinone, and the reaction mixture was stirred at room temperature for 24 h. The solution was poured into saturated aqueous sodium hydrogen carbonate, and the product was extracted with ethyl acetate. After the organic layer was dried with anhydrous magnesium sulfate, the solvent was removed by evaporation. The crude solid was purified by column chromatography (silica gel, chloroform as eluent) and finally recrystallized from methanol to yield 0.40 g (44%) of an orange solid. ^{1}H NMR ($CDCl_3$, δ, ppm): 1.46−1.94 (m, 8H), 2.74 (s, 3H), 3.65 (t, $J = 6.3$ Hz, 3H), 3.97 (t, $J = 6.3$ Hz, 3H), 6.87 (d, $J = 8.6$ Hz, 2H), 7.26−7.69 (m, 5H), 8.00 (d, $J = 8.7$ Hz, 2H), 8.36 (d, $J = 8.8$ Hz, 2H). ^{13}C NMR: 17.38, 18.27, 25.65, 25.72, 28.48, 29.00, 64.55, 67.72, 87.96, 93.08, 114.54, 114.60, 115.35, 123.41, 124.65, 125.17, 127.90, 129.53, 133.17, 134.24, 136.43, 139.70, 148.47, 149.35, 155.90, 159.48, 167.43. MS (FAB): 525 (MH^+). Anal. Calcd for $C_{31}H_{31}N_3O_5$: C, 70.84; H, 5.95; N, 8.00. Found: C, 70.58; H, 6.01; N, 8.01.

Polymerization of Monomer 13. Compound **13** (0.30 g, 0.57 mmol) and AIBN (3.5 mg, 5.7 μmol) were dissolved in dry DMF (5 mL) and placed in a polymerization tube. After several freeze−pump−thaw cycles, the tube was sealed under high vacuum. Then, the tube was kept at 60 °C for 48 h. The resulting solution was cooled to room temperature and poured into 100 mL of methanol with vigorous stirring to precipitate the polymer. The polymer obtained was purified by repeated reprecipitation from DMF into a large excess of methanol and dried under vacuum for 48 h to yield 0.18 g of **P3TA** in 60% conversion.

Characterization of LCPs. NMR spectra were recorded in $CDCl_3$ with a Lambda-300 spectrometer. Mass spectra were obtained with a JMS-700 spectrometer with fast atom bombardment (FAB). Molecular weight of the polymer was determined by gel permeation chromatography (GPC; JASCO DG-980-50; column, Shodex GPC K802 + K803 + K804 + K805; eluent, chloroform) calibrated with standard polystyrenes. LC behavior and phase transition behavior were examined on an Olympus model BH-2 polarizing microscope equipped with Mettler hot-stage models FP-90 and FP-82. Thermotropic properties of LCPs were determined with a differential scanning calorimeter (Seiko I&E SSC-5200 and DSC220C) at a heating rate of 10 °C/min. At least three scans were performed for each sample to check reproducibility. Absorption spectra were recorded by a UV−vis absorption spectrometer (JASCO, V-550). The polarized IR spectra of the films were measured with an FT/IR spectrometer (Jasco, FT/IR-420).

Preparation of LCP Films. To obtain an oriented film, the LCP was dissolved in toluene, and then a small portion of the resultant solution was coated on a glass substrate with a polyimide alignment layer that had been rubbed to align mesogens by a barcoater method. Homogeneously aligned films were obtained after annealing. Thickness of the sample films was measured with a surface profiler (Veeco Instruments Inc., Dektak 3ST), and the surface roughness of the films was within ±5 nm. For the measurement of polarized IR spectra, we used calcium fluoride as a substrate, on which a

Table 1. Thermodynamic Properties and Molecular Weights of Polymers[a]

polymer	phase transition temp (°C)	M_n	M_w/M_n
P3AT	G 47 N 220 I	21 000	3.9
P3TA	G 53 N 207 I	26 000	1.8
P3TA-NO$_2$	G 58 N 201 I	28 000	1.7

[a] G, glassy; N, nematic; I, isotropic.

Table 2. Quantum Yield and Isomerization Ratios of Polymers in Toluene

polymer	Φ_{tc}/Φ_{ct}[a]	trans:cis[b]
P3AT	0.26	0.32:0.68
P3TA	0.24	0.29:0.71
P3TA-NO$_2$	0.01	0.93:0.07

[a] Irradiation wavelength at 366 nm. [b] The trans:cis ratio at the photostationary state.

polyimide alignment layer was coated and the alignment layer was rubbed to align mesogens.

Photoisomerization Behavior of LCPs. We employed Fischer's method to evaluate the trans−cis photoisomerization behavior of the azotolane moieties in the LCPs.[21] Monochromatic excitation light was obtained from a Xe lamp (Ushio Optical Modulex, SX-UI501XQ) through a monochromator (JASCO, CT-10). We produced two photostationary states by using two different excitation wavelengths—366 and 410 nm—and estimated the ratio of the trans−cis and the cis−trans photoisomerization.[22]

Thermal Cis−Trans Isomerization Behavior of LCPs. We observed a change in absorbance at the absorption maximum of the trans state in solution to evaluate the thermal cis−trans isomerization behavior of the azotolane moiety. The LCP solution in a cell was placed in an absorption spectrometer, and we irradiated the sample with UV light (at 366 nm, 3 mW/cm^2) for 10 min at various temperatures and measured the absorbance of the trans form as a function of time.

Measurement of the Value of Birefringence. The change in birefringence was measured by means of an apparatus already reported.[23] The LCP film was placed in a thermostated block and irradiated at 366 nm with a 500 W high-pressure mercury lamp through glass filters (Asahi Technoglass, UV-D36A + UV-35 + IRA-25). The transmittance of the probe beam from diode lasers at 830 and 1550 nm or a He−Ne laser (633 nm) through two crossed polarizers, with the sample film between them, was measured with a photodetector.

Results and Discussion

Characterization of the Polymers. Table 1 shows the molecular weight, the molecular weight distribution, and the phase transition temperature of the polymers prepared in this study. All the polymers showed very stable N phases in a broad temperature range, which is quite advantageous for photonic applications in the LC phase. Since tolane moieties have a long π-conjugation length, their structures behave as a long rodlike mesogen. Therefore, generally tolanes show stable LC phases compared with conventional LCs.[14−16]

Trans−Cis Photoisomerization Behavior of Azotolanes. **P3AT** and **P3TA** without donor−acceptor moieties showed their absorption due to the $\pi-\pi^*$ transition of the azobenzene moieties at around 390 nm (A and B in Figure 2). The absorbance at around 390 nm decreased upon photoirradiation at 366 nm due to the trans−cis photoisomerization of the azobenzene moieties. On the other hand, **P3TA-NO$_2$** with donor−acceptor moieties exhibited the absorption maximum at 407 nm (C in Figure 2). This result indicates that the maximum absorption shifts toward a longer wavelength region with an increase of the strength of the electron donor−acceptor pair due to an increase in the π-orbital energy level and a decrease in the π^*-orbital energy.

We evaluated trans:cis ratios at the photostationary state and quatum yield ratios of the polymers (Table 2). Since the cis isomers cannot be detected in a pure form, their absorption spectra must be calculated from the spectra of the photostationary trans−cis mixtures. We employed Fischer's method to accomplish this task.[21] The method utilizes the photostationary state relationship

$$\frac{[\text{cis}]}{[\text{trans}]} = \frac{\epsilon_t}{\epsilon_c}\frac{\phi_{tc}}{\phi_{ct}} \tag{1}$$

where ϵ_t and ϵ_c are molar absorptivities for the trans and cis isomers, respectively, at the excitation wavelength (λ_{ex}) and ϕ_{tc} and ϕ_{ct} are the quantum yields of trans−cis and cis−trans photoisomerization, respectively. The unknown spectrum of the cis isomers can be calculated from the two spectra in the photostationary state obtained for different λ_{ex}. In all LCPs, the values of [cis]/[trans] and ϵ_c at λ_{ex} = 366 and 410 nm were estimated by the method previously reported.[22] Then we finally obtained the quantum yield ratio by eq 1.

The value of ϕ_{tc}/ϕ_{ct} of **P3TA-NO$_2$** was smaller than those of **P3AT** and **P3TA**, and only 7% cis isomer was present in the photostaionary state of **P3TA-NO$_2$**. On the other hand, the contents of cis isomers in **P3AT** and **P3TA** were above 65%. These results also can be explained by the donor−acceptor effect; the lifetime of the cis isomers is so short in the donor−acceptor azotolanes.

It is worth mentioning here that we synthesized an azotolane compound, in which the nitro group was attached to the tolane moiety and examined its optical properties. It was found that

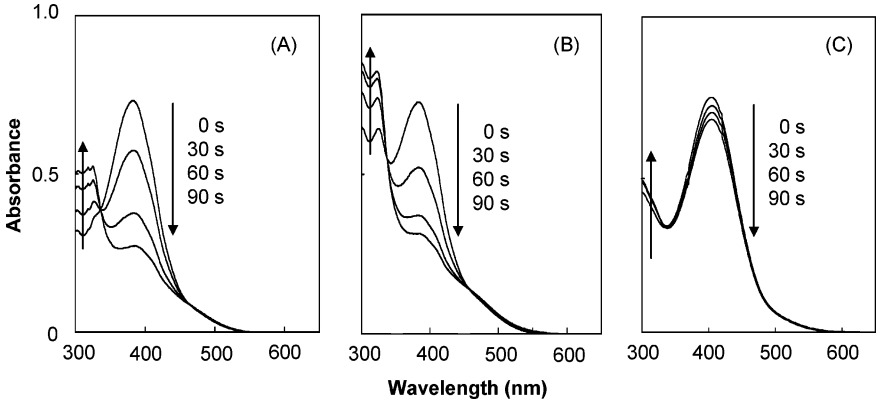

Figure 2. Change in the absorption spectra of LCPs in toluene upon irradiation at 366 nm (1.0 mW/cm^2): (A) **P3AT** (3.6×10^{-5} M); (B) **P3TA** (3.8×10^{-5} M); (C) **P3TA-NO$_2$** (3.3×10^{-5} M).

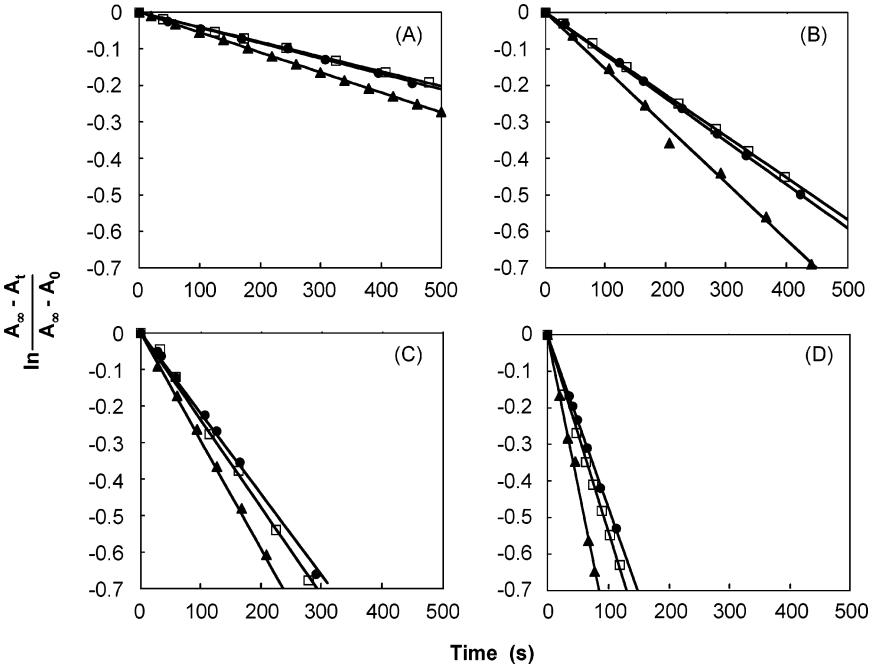

Figure 3. First-order plots for cis−trans thermal isomerization. (A) at 40 °C; (B) at 50 °C; (C) at 57 °C; (D) at 65 °C: (●) **P3AT**, (□) **P3TA**, and (▲) **P3TA-NO$_2$**.

Table 3. First-Order Rate Constants of the Thermal Cis−Trans Isomerization of the Azotolane Moieties in the LCPs

	k_{ct} (s^{-1}) × 10^{-2}			
polymer	40 °C	50 °C	59 °C	65 °C
P3AT	0.4	1.1	2.3	4.7
P3TA	0.4	1.2	2.5	5.2
P3TA-NO$_2$	0.5	1.6	3.0	8.3

the acceptor substituent gave no effect on the optical properties of the azobenzene moiety. In this study, therefore, we synthesized **P3TA-NO$_2$**, in which the nitro group is attached to the azobenzene moiety.

Thermal Cis−Trans Isomerization Behavior of Azotolanes. When all the LCPs irradiated at 366 nm were kept in the dark, cis−trans back-isomerization occurred thermally. We explored the effects of the structures of the azotolane moieties on the thermal cis−trans isomerization behavior. The differences in the three LCPs are the position of the tolane moiety in the azotolane mesogens and the terminal groups of the mesogens. The thermal isomerization behavior was analyzed by absorption spectroscopy. For the cis−trans isomerization, the first-order rate constant (k_{ct}) was determined by fitting the experimental data to the equation[24]

$$\ln\left(\frac{A_\infty - A_t}{A_\infty - A_0}\right) = -k_{ct}t \qquad (2)$$

where A_t, A_0, and A_∞ are the absorbances at the maxima wavelength of the $\pi-\pi^*$ transition at time t, time zero, and infinite time, respectively. Typical examples of the first-order plots according to eq 2 for the cis−trans isomerization of the azotolane moieties at various temperatures are shown in Figure 3. As shown in the figure, eq 2 gives a good fit to the thermal cis−trans isomerization. From the slope of the first-order plots, we obtained the value of k_{ct} in each LCP at various temperatures (Table 3).

The values of k_{ct} of **P3TA-NO$_2$** were larger than those of **P3AT** and **P3TA** at any temperature. This means that the thermal cis−trans isomerization of the donor−acceptor azotolane proceeds more effectively than that of the azotolanes without donor−acceptor pairs. On the other hand, the similar rate constant between **P3AT** and **P3TA** means that the position of the tolane moiety does not affect the thermal cis−trans back-isomerization behavior.

Table 4. Value of Birefringence of the LCP Films Aligned Homogeneously at 633, 830, and 1550 nm[a]

			Δn		
polymer	d (nm)	S	λ = 633 nm	λ = 830 nm	λ = 1550 nm
P3AT	320	0.42	0.39	0.33	0.30
P3TA	330	0.43	0.38	0.32	0.30
P3TA-NO$_2$	290	0.42	0.41	0.34	0.31

[a] d, film thickness, S, order parameter determined by polarized UV spectrometry; Δn, birefringence, λ, wavelength of the probe light.

Birefringence Dispersion of the Uniaxially Oriented LCP Films. Probe beams at various wavelengths (633, 830, and 1550 nm) were used to evaluate anisotropic properties of the LCP films. The LCP films were placed between a pair of crossed polarizers, and the transmittance of these probe beams was carefully measured. One can estimate the value of Δn of the LCP films by eq 3:[25−27]

$$T = \sin^2\left(\frac{\pi d\Delta n}{\lambda}\right) \qquad (3)$$

where d is the film thickness, Δn is the birefringence of the LCP film, T is the transmittance, and λ is the wavelength of the probe beam. Table 4 shows the values of Δn at various wavelengths. In the table are also included the value of the order parameters of the LCP films determined by polarized UV absorption spectroscopy.[8] All the LCP films showed very high values of Δn (above 0.3) at any wavelength examined between 633 and 1550 nm. Furthermore, the LCPs exhibited ordinary wavelength dispersion of Δn; with a decrease in wavelength the value of Δn increased due to resonant enhancement.

Photochemical Phase-Transition Behavior of LCPs. Effects of Structures of Azotolane Moieties. In **P3AT** and **P3TA**, the transmittance of the probe beam decayed immediately upon irradiation at 366 nm at 110 °C in an N phase (a and b in Figure

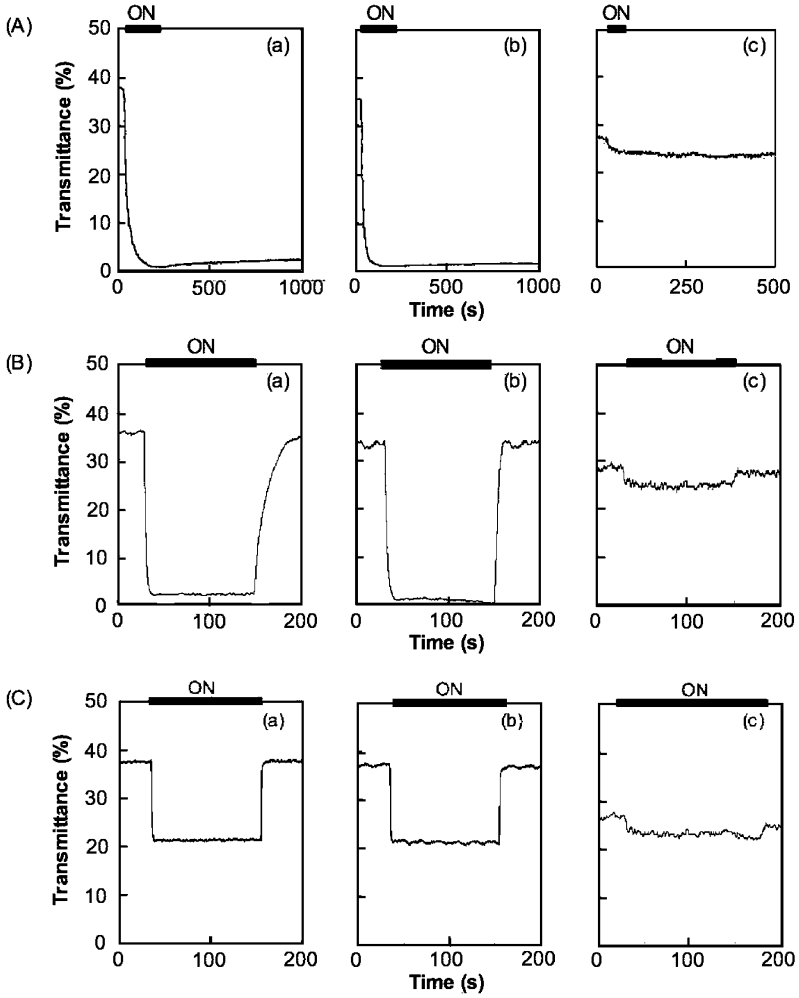

Figure 4. Change in transmittance of the LCP films at 633 nm upon irradiation at 366 nm. (A) at 45 °C (below T_g); (B) at 110 °C; (C) at 130 °C. (a) **P3AT**, (b) **P3TA**, and (c) **P3TA-NO$_2$**. Light intensity: 30 mW/cm^2.

4B). From the change in the transmittance, the calculated values of the change in Δn of the LCPs were above 0.35. This is attributed to the photochemical N−I phase transition of the LCPs due to trans−cis photoisomerization of the azobenzene moieties. Both LCPs showed almost the same behavior of the photochemical phase transition. On the other hand, little change in transmittance was observed in **P3TA-NO$_2$** with the donor−acceptor azotolane moiety (c in Figure 4B) upon irradiation at 366 nm. This is probably because the cis isomers of the azotolane moieties in **P3TA-NO$_2$** are unstable due to the donor−acceptor effect (as shown in Table 2), and the lifetime of the cis isomers in **P3TA-NO$_2$** is so short that they cannot induce the N−I phase transition. Similar effects have been already reported.[28] When all the irradiated LCP films were kept in the dark, the transmittance of the films recovered completely at 110 °C. This result inicates that the initial N phase is recovered when photoirradiation is ceased because the trans−cis azobenzene is restored thermally.

We also examined the photochemical phase transition behavior of the three LCPs at various temperatures. At 45 °C, which is below T_g of the polymers, the transmittance of the probe beam decayed upon irradiation at 366 nm; however, the recovery of the transmittance was not observed in all polymers, when they were kept in the dark. This is obviously due to the lack of the movement of the polymer segments below T_g, which prevents realignment of the azotolane moieties (Figure 4A).

At 130 °C, the photochemical N−I phase transition was not completed: the transmittance did not reach zero (or nearly zero) as shown in Figure 4C. This is due to shorter lifetimes of the cis forms at higher temperature, which would reduce the concentration of the cis isomers significantly and prevent the N−I phase transition. Furthermore, the photochemical N−I and the thermal I−N phase transitions could be induced repeatedly by irradiation of UV light at 110 °C (Figure 5).

Next, we investigated the cooperative motion of the tolane moieties in the azotolane groups induced by photoisomerization of the azobenzene. We measured the change in anisotropy of the tolane moieties by polarized IR spectroscopy, as shown in Figure 6. The transmittance band at 2208 cm^{-1} is attributed to the stretching vibration of the C≡C bond of the nonphotoactive tolane moiety. Before irradiation of UV light, the azotolane moieties were aligned parallel to the rubbing direction. Therefore, the intensity of the C≡C band was maximum when it was parallel to the rubbing direction and minimum when the polarization direction of the beam was perpendicular to the rubbing direction. One can see that not only the difference in the bands of the benzoic rings (1600, 1512, and 1251 cm^{-1}) but also that of the C≡C bond decreased significantly after irradiation. This means that the photochemical N−I phase transition has caused a cooperative motion of the tolane moieties in the azotolane groups coupled with the trans−cis isomerization of the azobenzene moiety and disorganizes the homogeneous alignment.

Optical Switching Behavior of the LCP Film at 1550 nm. In the near-infrared region, particularly the telecommunication wavelength (1550 nm), there have been studies on the elec-

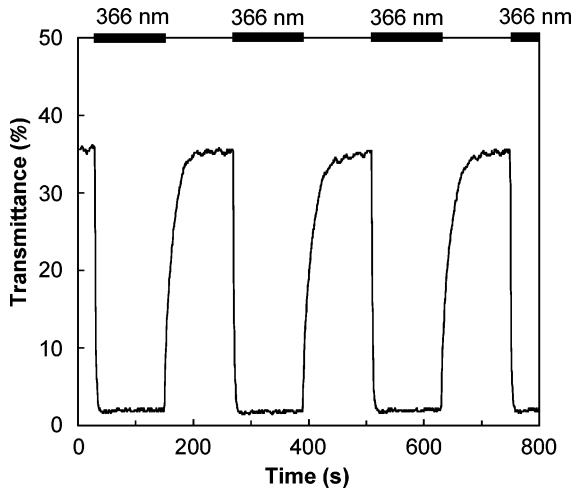

Figure 5. Photochemical N−I phase transition upon irradiation at 366 nm and thermal I−N phase transitions of the **P3AT** film probed at 633 nm. Photoirradiation at 366 nm (30 mW/cm^2) was performed at 110 °C.

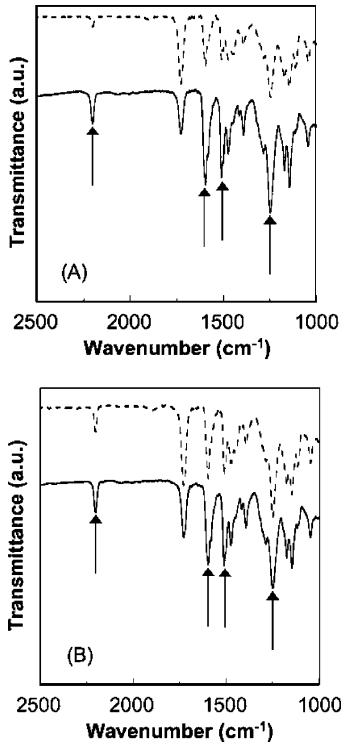

Figure 6. Polarized IR spectra of the **P3AT** film: (A) before irradiation; (B) after irradiation at 366 nm (30 mW/cm^2) for 1 min. Spectra were measured with polarized IR beam parallel (—) and perpendicular (···) to the rubbing direction.

trooptical and optical responses of LCs.[29,30] In the long wavelength region, the retardation of LCs, $d\Delta n$, should be increased to acquire the required phase change. Therefore, LCs having high Δn are expected to enhance the change in the phase of the beam.

We examined the optical switching behavior of the **P3AT** film at 1550 nm (Figure 7). Before irradiation of the pumping beam, the value of transmittance through the crossed polarizers was less than 5%. This is obviously because the transmittance decreases with an increase in the wavelength as eq 3 predicts. The transmittance decayed upon photoirradiation and recovered smoothly when the pumping light was turned off. From the change in transmittance of the probe beam, the calculated value of the change in Δn of the LCP film was about 0.2. As

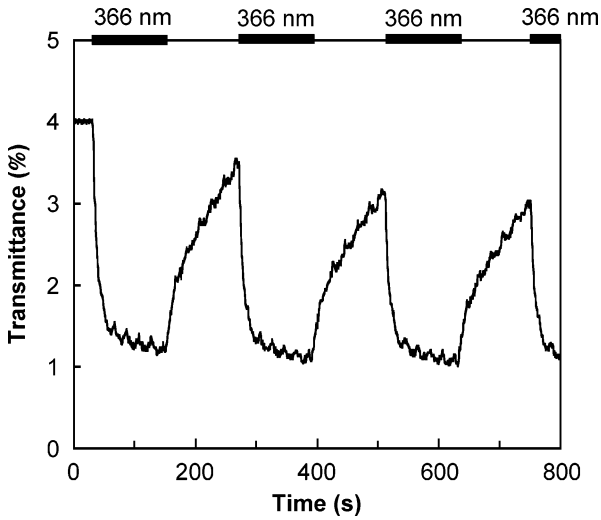

Figure 7. Photochemical N−I phase transition upon irradiation at 366 nm and thermal I−N phase transitions of the **P3AT** film probed at 1550 nm. Photoirradiation at 366 nm (30 mW/cm^2) was performed at 110 °C.

mentioned above, this optical switching behavior of the LCP film is caused by the N−I and I−N phase transition of the azotolane moieties. Recently, several tolane derivatives exhibiting high Δn have been intensively studied because high Δn is quite useful to reduce cell gaps of LC displays, which is advantageous to achieve fast response to the change in the electric field.[14,15] However, to the best of our knowledge, no report has been published on the change in Δn in the tolanes by external stimuli. In this study, we have demonstrated that the azotolane LCPs exhibiting high Δn enable us to control the light at the technologically important telecommunication wavelength by the photochemical phase transition induced by UV light.

Conclusion

In this study, we have synthesized novel azotolane LCPs and investigated the effects of the position of the tolane moiety in the azotolane group and that of the donor−acceptor substituent on the photochemical phase transition. All homogeneously aligned LCP films showed a very high value of Δn in the wide wavelength range, and the LCP films without donor−acceptor pairs exhibited a large change in Δn (>0.35 at 633 nm) repeatedly by the photochemical phase transition. Although the cis−trans back-isomerization of the LCP with the donor−acceptor azotolane moieties in solution was faster than that of LCPs having no donor−acceptor groups, the film of the donor−acceptor LCP still showed a little change in Δn by the photochemical N−I phase transition. Furthermore, we have presented photoswitching behavior, indicating a large change in Δn even at the telecommunication wavelength (1550 nm) by the photochemical phase transition induced by UV light. The LCPs, in which a very large change in Δn can be induced in the 633−1550 nm wavelength range, are promising materials for integrated photonic device application of optical memory and of optical switching.

References and Notes

(1) (a) Natansohn, A.; Rochon, P. *Chem. Rev.* **2002**, *102*, 4139. (b) Freiberg, S.; Lagugne-Labarthet, F.; Rochon, P.; Natansohn, A. *Macromolecules* **2003**, *36*, 2680. (c) Cojocariu, C.; Rochon, P. *J. Mater. Chem.* **2004**, *14*, 2909. (d) Wu, Y.; Natansohn, A.; Rochon, P. *Macromolecules* **2004**, *37*, 6090.

(2) (a) Shi, Y.; Steier, W. H.; Yu, L.; Chen, M.; Dalton, L. R. *Appl. Phys. Lett.* **1991**, *18*, 1131. (b) Chen, M.; Yu, L.; Dalton, L. R.; Shi, Y.; Steier, W. H. *Macromolecules* **1991**, *24*, 5421.
(3) Song, O. K.; Wang, C. H.; Pauley, M. A. *Macromolecules* **1997**, *30*, 6913.
(4) Dhanabalan, A.; Mendonca, C. R.; Balogh, D. T.; Misoguti, L.; Constantino, C. J. L.; Giacometti, J. A.; Zilio, S. C.; Oliveira, O. N. *Macromolecules* **1999**, *32*, 5277.
(5) Ikeda, T. *J. Mater. Chem.* **2003**, *13*, 2037.
(6) Ikeda, T.; Tsutsumi, O. *Science* **1995**, *268*, 1873.
(7) Shishido, A.; Tsutsumi, O.; Kanazawa, A.; Shiono, T.; Ikeda, T.; Tamai, N. *J. Am. Chem. Soc.* **1997**, *119*, 7791.
(8) (a) Wu, Y.; Demachi, Y.; Tsutsumi, O.; Kanazawa, A.; Shiono, T.; Ikeda, T. *Macromolecules* **1998**, *31*, 349. (b) Wu, Y.; Demachi, Y.; Tsutsumi, O.; Kanazawa, A.; Shiono, T.; Ikeda, T. *Macromolecules* **1998**, *31*, 1104. (c) Wu, Y.; Demachi, Y.; Tsutsumi, O.; Kanazawa, A.; Shiono, T.; Ikeda, T. *Macromolecules* **1999**, *32*, 3951.
(9) (a) Bobrovsky, A. Yu.; Pakhomov, A. A.; Zhu, X.-M.; Boiko, N. I.; Shibaev, V. P.; Stumpe, J. *J. Phys. Chem. B* **2002**, *106*, 540. (b) Zebger, I.; Rutloh, M.; Hoffmann, V.; Stumpe, J.; Siesler, H. W.; Hvilsted, S. *J. Phys. Chem. A* **2002**, *106*, 3454. (c) Rosenhauer, R.; Kozlovsky, M. V.; Stumpe, J. *J. Phys. Chem. A* **2003**, *107*, 1441. (d) Rosenhauer, R.; Fischer, Th.; Stumpe, J.; Gimenez, R.; Pinol, M.; Serrano, J. L.; Vinuales, A.; Broer, D. *Macromolecules* **2005**, *38*, 2213.
(10) Hagen, R.; Bieringer, T. *Adv. Mater.* **2001**, *13*, 1805.
(11) Sabi, Y.; Yamamoto, M.; Watanabe, H.; Bieringer, T.; Haarer, D.; Hagen, R.; Kostromine, S. G.; Berneth, H. *Jpn. J. Appl. Phys.* **2001**, *40*, 1613.
(12) Yoneyama, S.; Yamamoto, T.; Tsutsumi, O.; Kanazawa, A.; Shiono, T.; Ikeda, T. *Macromolecules* **2002**, *35*, 8751.
(13) Okada, S.; Matsuda, H.; Masaki, A.; Nakanishi, H.; Abe, T.; Ito, H. *Jpn. J. Appl. Phys.* **1992**, *31*, 365.
(14) (a) Sekine, C.; Iwakura, K.; Konya, N.; Minami, M.; Fujisawa, K. *Liq. Cryst.* **2001**, *28*, 1361. (b) Sekine, C.; Iwakura, K.; Konya, N.; Minami, M.; Fujisawa, K. *Liq. Cryst.* **2001**, *28*, 1375. (c) Sekine, C.; Iwakura, K.; Konya, N.; Minami, M.; Fujisawa, K. *Liq. Cryst.* **2002**, *29*, 355.
(15) Hird, M.; Toyne, K. J.; Goodby, J. W.; Gray, G. W.; Minter, V.; Tuffin, R. P.; McDonnell, D. G. *J. Mater. Chem.* **2004**, *14*, 1731.
(16) Gauza, S.; Wen, C. H.; Wu, S. T.; Janarthanan, N.; Hsu, C. S. *Jpn. J. Appl. Phys.* **2004**, *43*, 7634.
(17) Yang, Y.; Li, H.; Wang, K.; Wen, J. *Liq. Cryst.* **2001**, *28*, 375.
(18) Okano, K.; Shishido, A.; Tsutsumi, O.; Shiono, T.; Ikeda, T. *Proc. SPIE* **2003**, *139*, 5213.
(19) Shibaev, V. P.; Kostromin, S. G.; Plate, N. A. *Eur. Polym. J.* **1982**, *18*, 651.
(20) Angeloni, A. S.; Caretti, D.; Carlini, C.; Chiellini, E.; Galli, G.; Altomare, A.; Solaro, R. *Liq. Cryst.* **1989**, *4*, 513.
(21) Fischer, E. *J. Phys. Chem.* **1967**, *71*, 3704.
(22) Rau, H.; Greiner, G.; Gauglitz, G.; Meier, H. *J. Phys. Chem.* **1990**, *94*, 6523.
(23) Ikeda, T.; Horiuchi, S.; Karanjit, D. B.; Kurihara, S.; Tazuke, S. *Macromolecules* **1990**, *23*, 42.
(24) Sasaki, T.; Ikeda, T.; Ichimura, K. *Macromolecules* **1993**, *26*, 151.
(25) Zilker, S. J.; Beiringer, T.; Haarner, D.; Stein, R. S.; Egmond, J. W.; Kostromine, S. G. *Adv. Mater.* **1998**, *10*, 855.
(26) Stracke, A.; Wendorff, J. H.; Mahler, J.; Rafler, G. *Macromolecules* **2000**, *33*, 2605.
(27) Todorov, T.; Nikolova, L.; Tomova, N. *Appl. Opt.* **1984**, *23*, 4309.
(28) Tsutsumi, O.; Demachi, Y.; Kanazawa, A.; Shiono, T.; Ikeda, T.; Nagase, Y. *J. Phys. Chem. B* **1998**, *102*, 2869.
(29) Collings, N.; Bouvier, M.; Züger, B.; Grupp, J. *Mol. Cryst. Liq. Cryst.* **1998**, *320*, 277.
(30) Khoo, I. C.; Ding, J. *Appl. Phys. Lett.* **2002**, *81*, 2496.

MA0512814